The impact of climate change on water and energy security

The impact of climate change on water and energy security

Mohammad Reza Goodarzi, Hamed Vagheei and Rabi H. Mohtar

ABSTRACT

The interdependent fundamental systems, water and energy, face abundant challenges, one of which is climate change, which is expected to aggravate water and energy securities. The hydropower industry's benefits have led to its development and growth around the world. Nonetheless, climate change is expected to disturb the future performance of hydropower plants. This study looks at the Seimareh Hydropower Plant to assess the potential vulnerability of hydropower plants to climate change. Results indicate that climate change will affect the area's hydrological variables and suggest an increase in temperatures and decrease in precipitation during a 30-year future period (2040–2069). It is predicted that Seimareh Dam's inflow will decrease by between 5.2% and 13.4% in the same period. These hydrological changes will affect the Seimareh plant's performance: current predictions are that the total energy produced will decrease by between 8.4% and 16.3%. This research indicates the necessity of considering climate change impacts in designing and maintaining hydraulic structures to reach their optimal performance.

Key words | climate change, hydropower, Seimareh River basin, water and energy security

Mohammad Reza Goodarzi (corresponding author)
Department of Civil Engineering,
Yazd University,
Yazd,
Iran
and
WEF Nexus Research Group, Department of Biological and Agricultural Engineering,
Texas A&M University,
College Station, TX,
USA
E-mail: *goodarzimr@yazd.ac.ir*

Hamed Vagheei
Department of Environment, Land and Infrastructure Engineering,
Polytechnic University of Turin,
Turin,
Italy

Rabi H. Mohtar
Department of Biological and Agricultural Engineering,
Texas A&M University,
College Station, TX,
USA
and
Faculty of Food and Agricultural Sciences,
American University of Beirut,
Beirut,
Lebanon

HIGHLIGHTS

- This study looks at the Seimareh Hydropower Plant to assess the potential vulnerability of hydropower plants to climate change.
- It is predicted that Seimareh Dam's inflow will decrease by between 5.2% and 13.4% in the same period.
- These hydrological changes will affect the Seimareh plant's performance: current predictions are that the total energy produced will decrease by between 8.4% and 16.3%. This research indicates the necessity of considering climate change impacts in designing and maintaining hydraulic structures to reach their optimal performance.

INTRODUCTION

Climate change, a major global threat, has led to water and energy insecurity (Maas *et al.* 2012). Every continent suffers from water scarcity; it is predicted that by 2030, nearly half of the world's population will experience high water stress conditions, and these will likely impact energy security (Halstead *et al.* 2014). Unfortunately, while climate change will continue to have considerable impact on water and energy resources, the majority of our communities have little or no resilience to changing climate. Therefore, it seems necessary that various sectors of a community including the private sector, the public sector, and civil society work together to develop innovative approaches to mitigate the impacts of climate change on these essential resources (Mohtar 2017). Growing evidence of the effects of climate change on the planet has led to increasing interest in determining its potential impact on various sectors of the economy such as the hydropower industry,

doi: 10.2166/ws.2020.150

which has played a significant role in renewable and clean energy in the overall world energy supply in recent years. Nonetheless, climate change is predicted to have impacts on water resources leading to disturbance in hydropower generation (Vicuña *et al.* 2011; Meng *et al.* 2020). It is anticipated that by 2070, the hydropower potential for the whole of Europe will decline by 6%. Further, a 20–50% drop in hydropower potential is predicted for the Mediterranean region. Nevertheless, northern and eastern Europe are expected to actually increase their hydropower potential by 15–30%, while western and central Europe are expected to remain stable (Lehner *et al.* 2005). Northern Quebec's hydropower would likely benefit from higher precipitation, while hydropower in southern Quebec would likely be affected by lower water levels (Bates *et al.* 2008). A study conducted in California indicates that climate change is not anticipated to have much impact on the capacity of the two hydropower systems to generate energy when demand is at its peak. However, these systems could experience a drop in both energy generation and associated revenues (Vicuña *et al.* 2011). A report of the United States Department of Energy (2013) provides an analysis of potential climate change effects across four of the Power Marketing Administration regions. In the near-term period (2010–2024), the mean change in annual hydropower generation for the Bonneville Area is estimated to be an increase of 2% relative to the historic mean generation from 1989 to 2008, while in the mid-term period (2025–2039), the mean change in annual generation for this region is projected to be an increase of 3.3%. The report predicts that mean projected changes in annual generation for the Western Area will be an increase of 22% in the near-term and an increase of 20% in the mid-term. The mean projections for hydropower generation in the Southwestern Area indicate a 1.8% reduction in the near term and a 7.7% reduction in the mid-term period. For the Southeastern Area, the mean projected change in annual hydropower production is a 3.6% increase in the near-term period and almost no change in the mid-term period (USDOE 2013). The main results of the study conducted on the Valle d'Aosta Region in Italy predict a reduction of 10% in electricity production, despite the total quantity of water not being expected to change significantly (Maran *et al.* 2014). Another study performed on hydropower production of the Toce Alpine River Basin in Italy indicates an increase in hydropower production (Ravazzani *et al.* 2016). In Africa, results indicate increase in hydropower production in the Niger and Kwanza River Basins (Hamududu & Killingtveit 2016; Oyerinde *et al.* 2016) and hydropower production reduction in the Zambezi River Basin (Spalding-Fecher *et al.* 2017). Using a case study of the Rio Jubones Basin in Ecuador, Hasan & Wyseure (2018) suggested that hydropower generation would be affected due to the possible changes in seasonal flow regimes. Climate change is also expected to significantly reshape the hydropower industry in California (Forrest *et al.* 2018). While Boadi & Owusu (2019) suggest that climate variability affects Ghana's hydropower generation negatively through its effects on rainfall and ENSO, climate change is expected to have positive impacts on hydropower production in Sumatra, a tropical island in Indonesia (Meng *et al.* 2020). Various performed studies on China also indicate that hydropower systems in different regions of the country would be affected by climate fluctuations (Fan *et al.* 2020; Liu *et al.* 2020; Qin *et al.* 2020). Table 1 presents a summary of studies assessing impacts of climate change on hydropower systems.

Various studies demonstrate that optimized performance of hydraulic structures in the future relies on attention to climate change impacts. Obviously, the majority of relevant studies have been performed in Europe and the USA. Hence, this study uses the Seimareh Dam and Hydropower Plant to understand climate change impacts on hydropower production in western Asia. One important issue in climate modeling is the uncertainty principle of emission scenarios and climate models. Thus, the present study uses various emission scenarios and climate models to determine future water availability in the Seimareh River Basin, and to understand the possible vulnerability of Seimareh Hydropower Plant in the face of climate change.

METHODS

Climate conditions during the period 2040–2069 were predicted for the study area using general circulation models under various emission scenarios; the outputs of these models are downscaled by the Statistical DownScaling Model (SDSM). The river flow is simulated by the HEC-HMS hydrological model, and the Water Evaluation and Planning System (WEAP) model is used to simulate reservoir operation and calculate the amount of hydropower

Table 1 | Summary of relevant studies assessing climate change impacts on hydropower production

Study	Models/scenarios used	Location	Key results
Vicuña *et al.* (2011)	VIC model; LP optimization model; six GCMs under A2 and B1 emission scenarios	The Upper American River Project (UARP) and the Big Creek System, California, USA	• Increase in temperature • Decrease in precipitation • The average system power capacity in August (peak time) is reduced by a maximum of 0.6%
USDOE (2013)	VIC model; GCM: CCSM3; RCM: RegCM3; A1B emission scenario	Four of the Power Marketing Administration regions (Bonneville, Southeastern Area, Western Area, Southwestern Area), USA	• Increase in temperature • Changes in precipitation pattern • Increase in energy production for Bonneville, Western Area and Southeastern Area • Energy generation reduction for Southwestern Area
Maran *et al.* (2014)	TOPKAPI model; SOLARIS; GCM: ECHAM; RCMs: REMO and RegCM; A1B emission scenario	The Valle d'Aosta Hydropower System, Italy	• Expected changes in the precipitation pattern • A statistically significant decrease in overall hydropower production: 10% of the annual production of the whole system (equivalent to 200 GWh)
Ravazzani *et al.* (2016)	FEST-WB model; BPMPD solver; GCM: ECHAM5; RCMs: REMO and RegCM3; A1B emission scenario	Toce River Basin, Italy	• Increase of temperature • Increase of mean annual precipitation • Increase in hydropower production (11–19%)
Oyerinde *et al.* (2016)	IHACRES; ARMAX; eight GCMs; RCM: SMHI-RCA; RCP 4.5 and RCP 8.5 emission scenarios	Kainji Hydroelectric Dam, Niger Basin, West Africa	• Increase in temperature • Increase in precipitation • Increase in PET • Increase in hydropower production
Hamududu & Killingtveit (2016)	HBV model; nMAG; five GCMs; ESD; A1B and B2 emission scenarios	Kwanza River Basin, Angola	• Increase in temperature • For precipitation: a decrease in the 2020s, and then an increase towards the end of the 21st century • Increase in inter-annual variability of precipitation • Increase in hydropower production in the basin by up to 10%
Lobanova *et al.* (2016)	SWIM model; ISI-MIP; RCP 4.5 and RCP 8.5 emission scenarios	Tagus River Basin, 3 hydropower reservoirs in Spain and Portugal	• Decrease in inflows to reservoirs • Strong decrease in hydropower production in all three reservoirs (10–60%)
Spalding-Fecher *et al.* (2017)	WEAP; LEAP; SSPs emission scenarios	Zambezi River Basin, southern Africa	• Energy production reduction by about 10–20% under a drying climate • Only marginal increases in generation with a plausible wetting climate

(*continued*)

Table 1 | continued

Study	Models/scenarios used	Location	Key results
Turner *et al.* (2017)	WaterGAP; three GCMs under A2 and B1 emission scenarios	Global	• Energy production responds non-linearly to climate change • The Balkans region emerges as most vulnerable to power production losses • A significant increase in total electrical production in a handful of countries in Scandinavia and Central Asia
Forrest *et al.* (2018)	VIC model; four GCMs under RCP 4.5 and RCP 8.5 emission scenarios	California, USA	• Temporal shift in runoff and hydropower generation • Increased chance of reservoir spillage and lost generation potential due to increase in winter and spring runoffs • Decrease in spinning reserve bidding potential
Hasan & Wyseure (2018)	SWAT; three climate change scenarios for the future period (2045–2065)	Rio Jubones Basin, Ecuador	• Changes in seasonal flow regimes • Changes in hydropower potential • Wet season: increase in rainfall, streamflow and hydropower generation • Dry season: decrease in rainfall, streamflow and hydropower generation
Meng *et al.* (2020)	PRC-GLOBWB model; four GCMs under RCP 2.6 and RCP 6.0 emission scenarios and global warming levels of 1.5 and 2 °C	Sumatra, Indonesia	• Positive impacts on hydropower generation under both global warming levels • Higher hydropower generation under global warming of 1.5 °C • Higher reduction in CO_2 emissions under global warming of 1.5 °C
Qin *et al.* (2020)	SWAT; five GCMs under RCP 2.6, RCP 4.5 and RCP 8.5 emission scenarios	The Three Gorges Reservoir, China	• Increase in precipitation • Increase in mean annual inflow (3.3–15.2%) • Increase in mean annual hydropower generation (0.9–8.1%)
This study	HEC-HMS; WEAP and energy module; GCMs: HadCM3, CGCM3 and CanESM2; SDSM; A2, B2, RCP 2.6, RCP 4.5 and RCP 8.5 emission scenarios	Seimareh Dam and Hydropower Plant, Iran	• Increase in temperature • Decrease in precipitation • Decrease in Seimareh Dam inflow (5.2–13.4%) • Decrease in energy production (8.4–16.3%)

production. See Appendix A (Supplementary Material) for the overall methodology applied in this study.

STUDY AREA AND DATA

Karkheh Basin, in the central and southwestern Zagros Mountains of western Iran, occupies about 50,764 km^2, and includes five sub–basins: Gamasiab, Qarasou, Seimareh, Kashkan and Southern Karkheh. The basin is located between 46° 06′E and 49° 10′E longitude and 30° 58′N and 34° 56′N latitude. The basins of Sirvan, Qezel–Owzan, and Qara–Chay Rivers lie to the north, the border river basins of Iran and Iraq to the west, and the Dez River Basin lies to the east and part of the west border of Iran in the south (Zahabiyoun *et al.* 2013). The mean annual precipitation in the Karkheh Basin varies from 150 mm in the southern part to 700 mm in the northern part. The mean annual temperature also ranges from 5 °C to 25 °C. From the perspective of the development of Karkheh Basin, several dams have various functions, including hydropower, agriculture and water transfer systems. The present research looks at the Seimareh Dam and Hydropower Plant, which is located in the Seimareh River Basin. The Seimareh River is formed by the confluence of the Qarasou and Gamasiab Rivers; its main branches are the Chardavol and Shiravan Rivers. The Seimareh Dam, in the northwest of Khuzestan and Ilam provinces, lies 40 km northwest of Darreh Shahr City and 106 km southeast of Ilam City (geographical coordinates: 47° 12′E longitude and 33° 17′N latitude). The mean annual precipitation in the Seimareh River Basin is about 442.7 mm for the 46-year period (1958–2003), while this value is about 425 mm at the Seimareh Dam. The temperature at the Seimareh Dam ranges from −6 °C to 51 °C with a mean annual value of 20.1 °C (IWPRDC 2008). River discharge data at Seimareh Dam was collected from Mahab Ghodss Company for the period between 1956 and 2005, and the mean annual river discharge is about 102.8 m^3/s during this period. Daily precipitation and temperature data (1971–2000) were collected from several stations (Table 2). Figure 1 shows the location of the study area, the Seimareh Dam and meteorological stations.

GENERAL CIRCULATION MODELS

Future climate prediction relies on computer numerical models known as general circulation models (GCMs) that simulate Earth's climate. GCMs provided by various research centers have significantly improved in recent decades (Wilby *et al.* 2004). In this study, three GCMs (CanESM2, CGCM3 and HadCM3) were assessed. After reviewing the three models according to two statistical indices: coefficient of determination (R^2), and Nash–Sutcliffe efficiency (NSE),

Table 2 | Summary of stations' data used in the study

Station name	Type of data	Longitude (°E)	Latitude (°N)	Elevation (masl[a])	Source
Pol Chehr	Precipitation	47° 26′ 00″	34° 20′ 00″	1,306	IWRMC[b]
Ghoorbaghestan	Precipitation	47° 15′ 00″	34° 14′ 00″	1,300	IWRMC
Holeylan–Seimareh	Precipitation, temperature	47° 15′ 00″	33° 44′ 00″	900	IWRMC
Holeylan–Jazman	Precipitation	47° 06′ 00″	33° 46′ 00″	950	IWRMC
Tang Siab	Precipitation	47° 12′ 22″	33° 23′ 25″	880	IWRMC
Gol Zard	Precipitation	47° 21′ 36″	33° 11′ 01″	680	IWRMC
Nazarabad	Precipitation	47° 26′ 03″	33° 10′ 21″	559	IWRMC
Vargach	Precipitation	46° 49′ 09″	33° 33′ 21″	783	IWRMC
Kermanshah	Temperature	47° 09′ 00″	34° 21′ 00″	1,318.6	IMO[c]
Seimareh Dam	Runoff	47° 12′ 00″	33° 17′ 00″	705	MGC[d]

[a]Metres above sea level.
[b]Iran Water Resources Management Company.
[c]Iran Meteorological Organization.
[d]Mahab Ghodss Company.

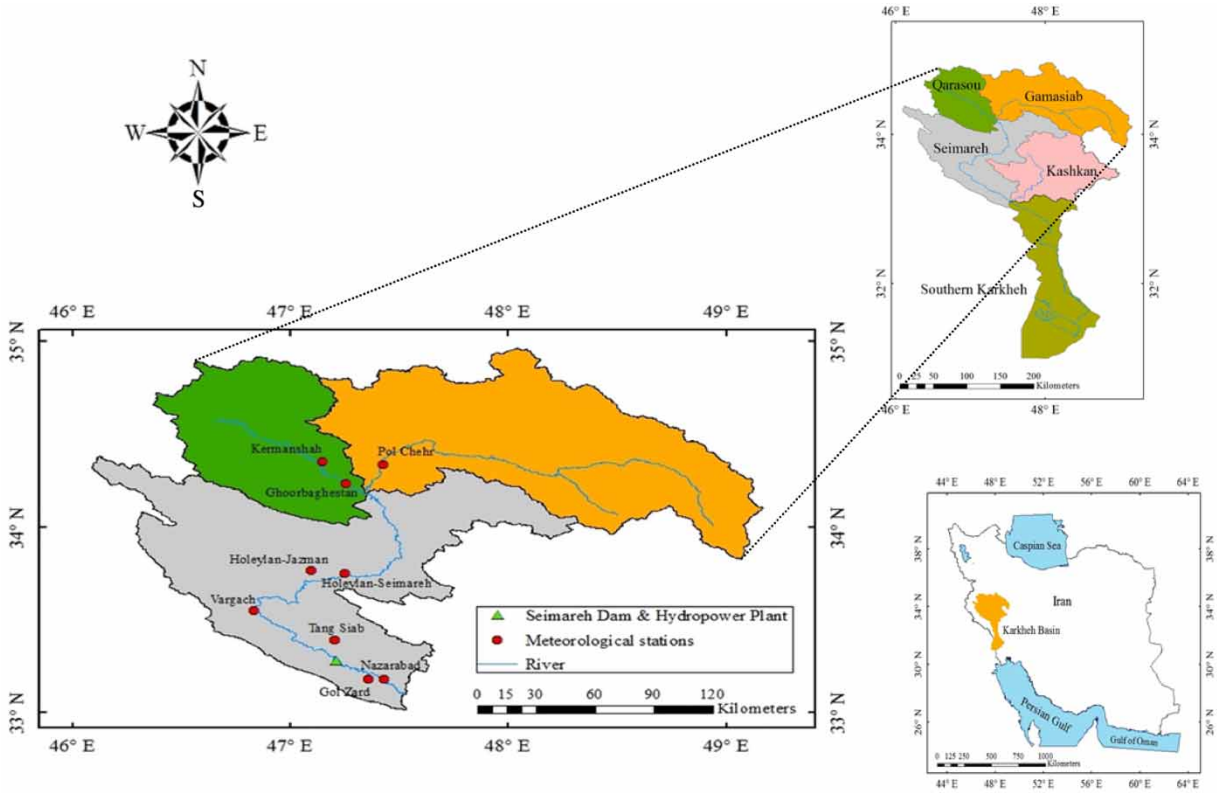

Figure 1 | The location of the study area, the Seimareh Dam, and meteorological stations.

the author found two models (HadCM3 and CanESM2) to be well-matched with the region of the study; these were used to assess the impacts of climate change.

EMISSION SCENARIOS

The greenhouse gas emission scenarios are used to provide an image of Earth's future based on the level of radiative force, technology, and socio-economic status (IPCC 2000; Collins *et al.* 2013). In this study, the five emission scenarios A2, B2, RCP2.6, RCP4.5, and RCP8.5 are used.

DOWNSCALING

The outputs of the GCMs are downscaled using statistical and dynamic methods. The Statistical DownScaling Model developed by Wilby *et al.* (2002) is used in the present study to downscale the GCM outputs.

HYDROLOGICAL MODEL

In the present study, the HEC–HMS (Hydrologic Engineering Center–Hydrologic Modeling System) hydrological model was employed. The HMS model is applied for modeling hydrological systems and analyzing the geographic information system (HEC 2000). In this study, the Soil Moisture Accounting (SMA) method (see Appendix B, Supplementary Material) is used to calculate losses, and the Clark unit hydrograph is used to calculate runoff amounts.

WEAP MODEL

The Water Evaluation and Planning System is appropriate for municipal and agricultural systems, single sub-basins or complex river systems. WEAP that can address a wide range of issues was used in this study to simulate reservoir operations and to calculate hydropower production. For each dam, in addition to five parameters (min turbine

flow, max turbine flow, tailwater elevation, plant factor, and generating efficiency), other parameters are introduced into WEAP in the format of Equations (1)–(5), explained below.

$$Q_{\mathrm{d}} = \frac{P_{\mathrm{dep}} \times 1000}{9.81 \times \eta \times H_{\mathrm{d}}} \tag{1}$$

where Q_{d} is design flow (m^3/s), η is generating efficiency, P_{dep} is installed capacity of plant (MW), and H_{d} is design head (m).

$$H_{\mathrm{net}} = H_{\mathrm{t}} - TWL - H_{\mathrm{f}} \tag{2}$$

where H_{net} is net head (m), H_{t} is headwater at the beginning of the month (m), TWL is tailwater level (m), and H_{f} is the head loss (m).

$$Q_{\max} = \min\left(\frac{P_{\mathrm{dep}} \times 1000 \times Overload}{9.81 \times \eta \times H_{\mathrm{net}}},\ C_{Q_{\max}} \times Q_{\mathrm{d}}\right) \tag{3}$$

where $Q_{\max}$ is max flow (m^3/s), $C_{Q_{\max}}$ is the coefficient of max flow, and *Overload* is the coefficient of overload of the planet.

$$Q_{\mathrm{req}} = \min\left(\frac{P_{\mathrm{dep}} \times 1000}{9.81 \times \eta \times H_{\mathrm{net}}},\ Q_{\max}\right) \tag{4}$$

where Q_{req} is the required flow for producing energy (m^3/s). The required volume of water for producing energy is obtained by Equation (5):

$$\text{if: } C_{H_{\min}} \times H_{\mathrm{d}} \le H_{\mathrm{net}} \le C_{H_{\max}} \times H_{\mathrm{d}} \rightarrow V_{\mathrm{D}} = Q_{\mathrm{req}} \times PT \times N_{\mathrm{day}} \times 3600/10^6 \tag{5}$$

where $C_{H_{\min}}$ is the coefficient of min head, $C_{H_{\max}}$ is the coefficient of max head, V_{D} is the required volume of water for producing energy, PT is the number of peak times (hr), and N_{day} is the number of days of each month.

Due to the limitations of the WEAP model, the amount of productive energy is calculated according to the required water and reservoir level. For this purpose, a macro was created using Excel to control the WEAP model and provide a complete link between Excel and the WEAP model. After entering data, the WEAP model is run by the macro's command; required data are extracted; and hydropower calculations are performed (Loucks & van Beek 2005; Jalali *et al.* 2008; Sieber & Purkey 2015).

RESULTS AND DISCUSSION

SDSM performance

The SDSM model was used to downscale GCMs. The performance of the model was checked using three statistical indices: coefficient of determination (R^2), Nash–Sutcliffe efficiency (NSE) and root mean square error (RMSE). Two models (HadCM3 and CanESM2) well matched with the base period were used to achieve optimal results. Because of unsuitable results from some stations, including Holeylan–Jazman, Gol Zard and Vargach, data from these stations were neglected. The values of the used statistical indices for simulating monthly precipitation and temperature during the calibration and validation periods are shown in Table 3.

Future temperatures

Future temperatures were evaluated using the data of Kermanshah and Holeylan–Seimareh Stations: the maximum temperatures in the observed and future periods are shown in Table 4. The maximum temperature will increase under all scenarios: the lowest maximum temperature rise is 0.2 °C using the CanESM2 model under the RCP2.6 scenario for Kermanshah Station, and the highest maximum temperature rise is 1.2 °C using the CanESM2 model under the RCP8.5 scenario for Holeylan–Seimareh Station. Table 5 presents the minimum temperatures of these stations in the observed and future periods: the minimum temperature in both stations will increase in the future. The lowest minimum temperature rise is 0.2 °C using the CanESM2 model under the RCP2.6 scenario for Kermanshah Station and the highest minimum temperature rise is 1.3 °C using the CanESM2 model under the RCP8.5 scenario for Holeylan–Seimareh Station.

Figure 2 presents the monthly changes in the maximum temperature of Kermanshah and Holeylan–Seimareh Stations. Figure 3 presents the monthly changes in the minimum temperature for the future period. As is

Table 3 | Performance of the SDSM model during calibration and validation periods

		Calibration (1971–1985)			Validation (1986–2000)		
Station name	**Model**	R^2	**NSE**	**RMSE**	R^2	**NSE**	**RMSE**
Precipitation							
Pol Chehr	CanESM2	0.97	0.96	1.07	0.82	0.78	1.38
	HadCM3	0.97	0.94	1.11	0.77	0.75	1.7
Ghoorbaghestan	CanESM2	0.94	0.93	0.98	0.78	0.75	1.46
	HadCM3	0.89	0.87	1.34	0.91	0.84	1.46
Holeylan–Seimareh	CanESM2	0.95	0.92	1.34	0.64	0.58	1.23
	HadCM3	0.92	0.84	1.63	0.67	0.62	1.2
Tang Siab	CanESM2	0.86	0.82	1.33	0.76	0.62	1.62
	HadCM3	0.97	0.96	1.34	0.73	0.68	1.65
Nazarabad	CanESM2	0.96	0.96	1.08	0.74	0.7	1.44
	HadCM3	0.86	0.83	1.15	0.87	0.86	1.67
Maximum temperature							
Kermanshah	CanESM2	0.98	0.97	2.06	0.97	0.95	2.51
	HadCM3	0.98	0.96	1.9	0.97	0.95	2.54
Holeylan–Seimareh	CanESM2	0.97	0.96	1.65	0.95	0.93	2.6
	HadCM3	0.95	0.93	1.74	0.94	0.93	2.58
Minimum temperature							
Kermanshah	CanESM2	0.98	0.97	1.63	0.96	0.95	1.76
	HadCM3	0.98	0.97	1.61	0.97	0.95	1.81
Holeylan–Seimareh	CanESM2	0.96	0.95	1.07	0.96	0.94	1.8
	HadCM3	0.96	0.94	1.11	0.96	0.95	1.74

Table 4 | The mean annual maximum temperature of stations in the base and future periods (°C)

		Future period									
		CanESM2						HadCM3			
Station name	**Base period**	**RCP8.5**		**RCP4.5**		**RCP2.6**		**B2**		**A2**	
Kermanshah	22.5	23.5	+1	23.3	+0.8	22.7	+0.2	23.2	+0.7	23.5	+1
Holeylan–Seimareh	26.3	27.5	+1.2	27.1	+0.8	26.6	+0.3	27.1	+0.8	27.3	+1

Table 5 | The mean annual minimum temperature of stations in the base and future periods (°C)

		Future period									
		CanESM2						HadCM3			
Station name	**Base period**	**RCP8.5**		**RCP4.5**		**RCP2.6**		**B2**		**A2**	
Kermanshah	6.1	7.2	+1.1	7	+0.9	6.3	+0.2	6.8	+0.7	7	+0.9
Holeylan–Seimareh	9.5	10.8	+1.3	10.6	+1.1	9.9	+0.4	10.3	+0.8	10.6	+1.1

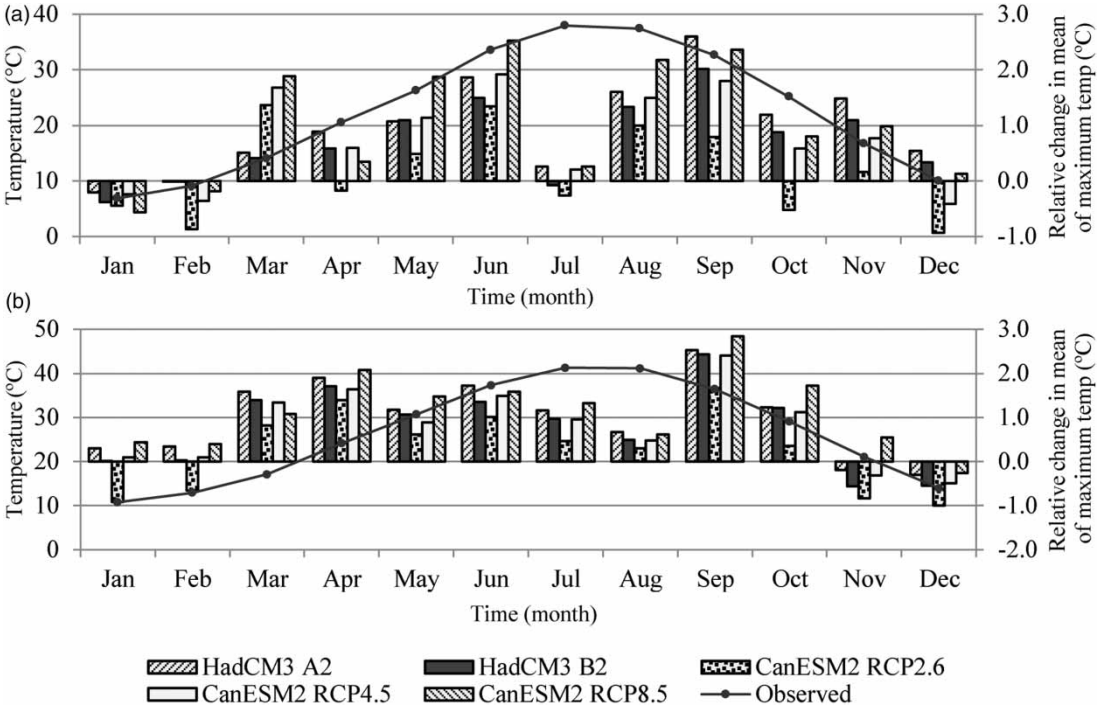

Figure 2 | Changes in the mean monthly maximum temperature: (a) Kermanshah and (b) Holeylan–Seimareh.

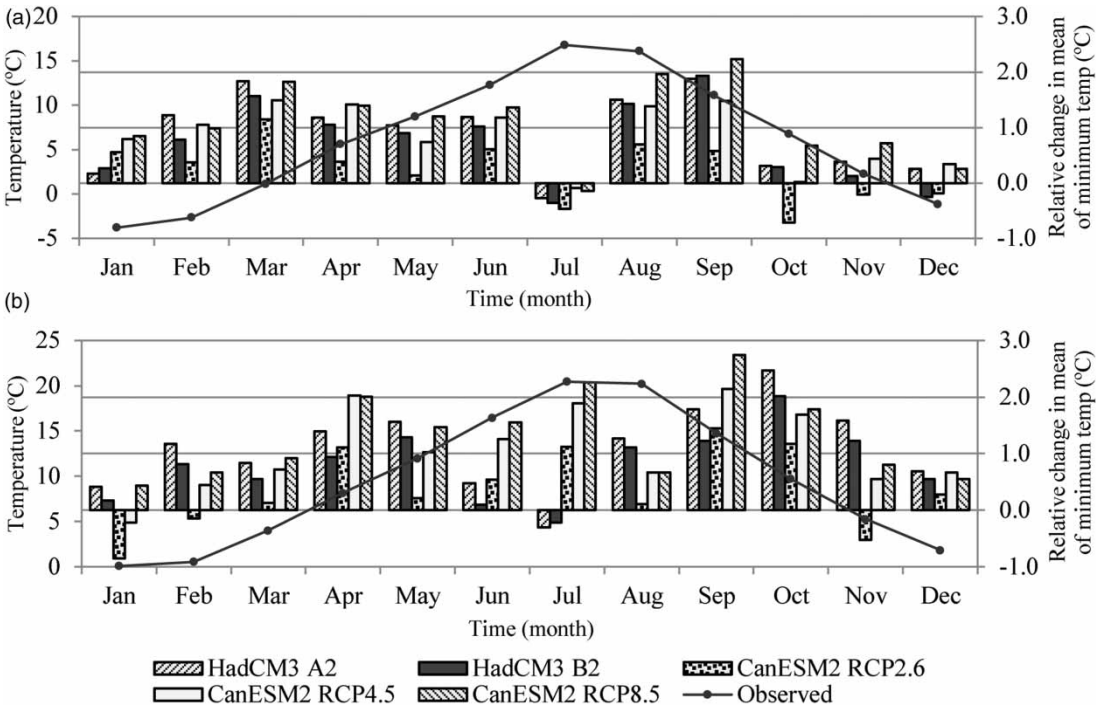

Figure 3 | Changes in the mean monthly minimum temperature: (a) Kermanshah and (b) Holeylan–Seimareh.

clear from these figures, the maximum and minimum temperatures of both stations will increase in most months; in only a few months and under some scenarios, temperatures will decrease. The line graphs in these figures represent the mean monthly temperature (maximum or minimum) for the observation period. Only the left axis is used to obtain temperature per month; bar graphs indicate the amount of temperature change according to various models and scenarios for the future period. The amount of temperature increase or decrease in this period is reflected using the right axis. The highest maximum temperature for Kermanshah Station was 38 °C (in July) and lowest maximum temperature was 9.6 °C (in January) in the observation period. The highest maximum temperature rise of Kermanshah Station occurs in September (2.6 °C); this rise is related to the HadCM3 model under the A2 scenario. The highest temperature reduction (December, 0.95 °C) is reflected in the CanESM2 model under the RCP2.6 scenario. Figure 2 also shows that the highest maximum temperature rise of Holeylan–Seimareh Station occurs in December (2.85 °C). Figure 3 presents the highest minimum temperature rise of Kermanshah (September, 2.25 °C) and Holeylan–Seimareh (September, 2.75 °C).

Future precipitation

Assessment of future precipitation used five stations: Pol Chehr, Ghoorbaghestan, Holeylan–Seimareh, Tang Siab, and Nazarabad. Table 6 shows precipitation amounts for these stations during the observation and future periods. The table reveals that the precipitation in the future period will remain unchanged only at Holeylan–Seimareh Station for the CanESM2 model under the RCP2.6 scenario. For all other stations, a reduction in the precipitation amount is predicted. The highest amount of precipitation reduction will occur at Tang Siab Station, with a projected decrease of 15.9%.

Figure 4 presents the monthly precipitation changes at the stations. Line graphs represent the amount of monthly precipitation in the observation period. Bar graphs provide the monthly precipitation changes for various models and scenarios.

Preparation of the HEC–HMS model

To determine the Seimareh Dam inflow, the daily precipitations for selected stations were used as input data in the hydrologic model; the Hargreaves–Samani equation was used to determine the amount of evapotranspiration. Initial values of parameters used in the calibration process were estimated based on available databases and published studies (IWPRDC 2008; Teymouri Moghadam *et al.* 2010; Ghafouri *et al.* 2013). In this simulation, the period 1987–1990 was considered as the calibration period and the period 1993–1996 as the validation period. Table 7 presents final calibrated parameters for different sub-basins. To compare the daily simulated and observed flows, the two statistical indices of NSE and R^2 were used (Table 8). Figure 5 indicates the results of the calibration and validation of the hydrologic model.

Table 6 | The mean annual precipitation of stations in the observation and future periods (mm)

		Future period									
		CanESM2						HadCM3			
Station name	Observation period	RCP8.5		RCP4.5		RCP2.6		B2		A2	
Pol Chehr	405.2	361	−10.9%	370.1	−8.7%	401.1	−1%	384.7	−5.1%	372.6	−8.1%
Ghoorbaghestan	397.9	352.2	−11.5%	367.5	−7.6%	385.1	−3.2%	382.9	−3.8%	366.4	−7.9%
Holeylan–Seimareh	350.5	324.8	−7.3%	339.4	−3.2%	350.5	–	345.6	−1.4%	337.2	−3.8%
Tang Siab	427.1	359.2	−15.9%	373.4	−12.6%	403.3	−5.6%	381.7	−10.6%	366.1	−14.3%
Nazarabad	355.5	330	−7.2%	336.9	−5.2%	347.5	−2.3%	342.4	−3.7%	332.9	−6.4%

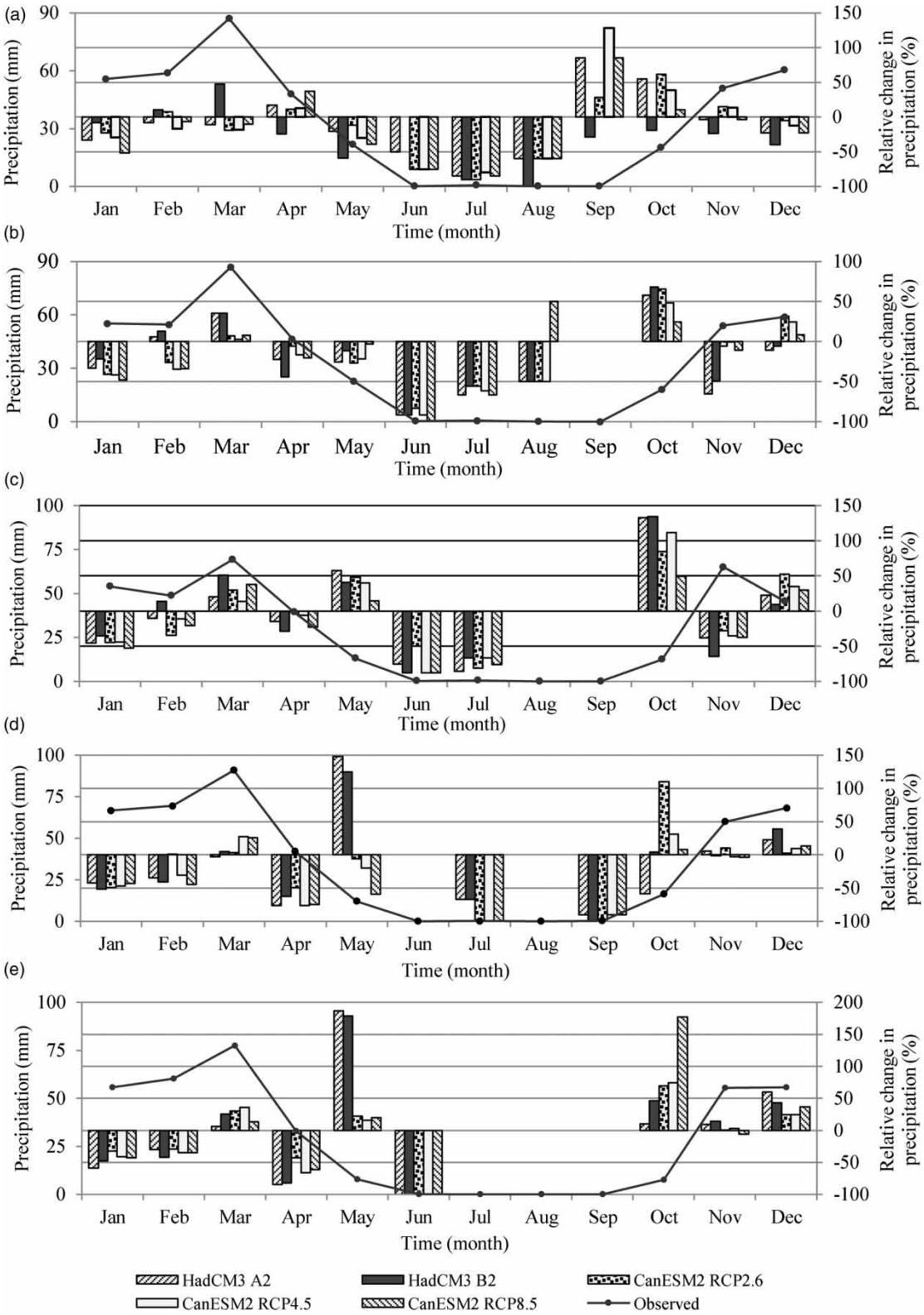

Figure 4 | The mean monthly precipitation changes: (a) Pol Chehr Station, (b) Ghoorbaghestan, (c) Holeylan–Seimareh, (d) Tang Siab, and (e) Nazarabad.

Table 7 | Calibrated parameters used in the HEC–HMS model for different sub-basins

Parameter	Qarasou	Gamasiab	Seimareh
Max canopy storage (mm)	1.3	1.3	1.2
Max surface storage (mm)	4.8	5	4.5
Max infiltration (mm/hr)	11	10	10
Impervious (%)	14	14	14
Soil storage (mm)	115	115	115
Tension storage (mm)	18	17.5	17.5
Soil percolation (mm/hr)	4.5	4	3.75
GW1 storage (mm)	85	85	85
GW1 percolation (mm/hr)	3.5	3	2
GW1 coefficient (hr)	400	400	400
GW2 storage (mm)	95	95	95
GW2 percolation (mm/hr)	0.08	0.05	0.04
GW2 coefficient (hr)	600	600	600
Time of concentration (hr)	25.5	28	35
Storage coefficient (hr)	53.5	74.5	85
Recession constant	0.98	0.98	0.99

Table 8 | The results of calibration and validation of the HEC–HMS model for simulating the daily inflow to Seimareh Dam

	Calibration period (1987–1990)		Validation period (1993–1996)	
Index	R^2	NSE	R^2	NSE
Amount	0.81	0.79	0.78	0.77

Future discharge

The Seimareh River streamflow was simulated using the HEC–HSM model. Table 9 shows the average annual river flow at Seimareh Dam for the 50–year observation period (1956–2005) and the future period (2040–2069). The table shows that the river flow in the future period will decrease in all scenarios and models, with the greatest river flow reduction shown in the CanESM2 model under the RCP8.5 scenario.

Figure 6 shows the monthly streamflow of Seimareh River at Seimareh Dam: the streamflow pattern of the river in the future period will change in some months of the year compared with the 50–year observation period. The inflow to Seimareh Dam in November, December, and January (mid-autumn to mid-summer) will increase; during February to June end (mid-winter to early summer) the inflow will decrease; and during July to October end (early summer to mid-autumn) the inflow will not change significantly.

Future hydropower production

Turner *et al.* (2017) assessed climate change impacts on global hydropower production (see Appendix C, Supplementary Material). They predicted that the mean change of hydropower production in Iran will be about −10.3%.

In the present study, the amount of energy produced by the Seimareh Hydropower Plant was assessed using the WEAP model. Table 10 shows energy production values during the 50-year observation period (1956–2005) and the future period (2040–2069). The total energy produced is expected to decrease under all scenarios. This reduction shows that climate change will influence hydrological conditions in the region, impacting the Seimareh Dam inflow and consequently, the performance of the Seimareh Hydropower Plant. Table 10 shows that the RCP2.6 scenario is the most optimistic, due to the inclusion of cases including lower population growth, use of renewable energies and high technologies, low greenhouse gas emissions, and exertion of environmentally friendly measures for future climate. In contrast, the RCP8.5 scenario is the most pessimistic among the scenarios due to high population growth, use of fossil and non-renewable fuels, low level of technological development, increase of greenhouse gas emissions, and lack of attention to environmental concerns for future climate conditions. Thus, scenario RCP2.6 predicts the least reduction of Seimareh hydropower production and scenario RCP8.5 predicts the highest amount of hydropower production in the future. According to official figures, electricity consumption per capita is about 2,900 kWh in Iran (Tavanir Organization 2016) and, as Table 10 shows, it is predicted that the vulnerability of Seimareh Hydropower Plant in the face of climate change will be considerable, since even in the most optimistic case, the amount of energy production will decrease by about 8.4% (70 GWh). In Iran, this value (8.4%) is sufficient power for about 24,000 people in a year. The worst-case

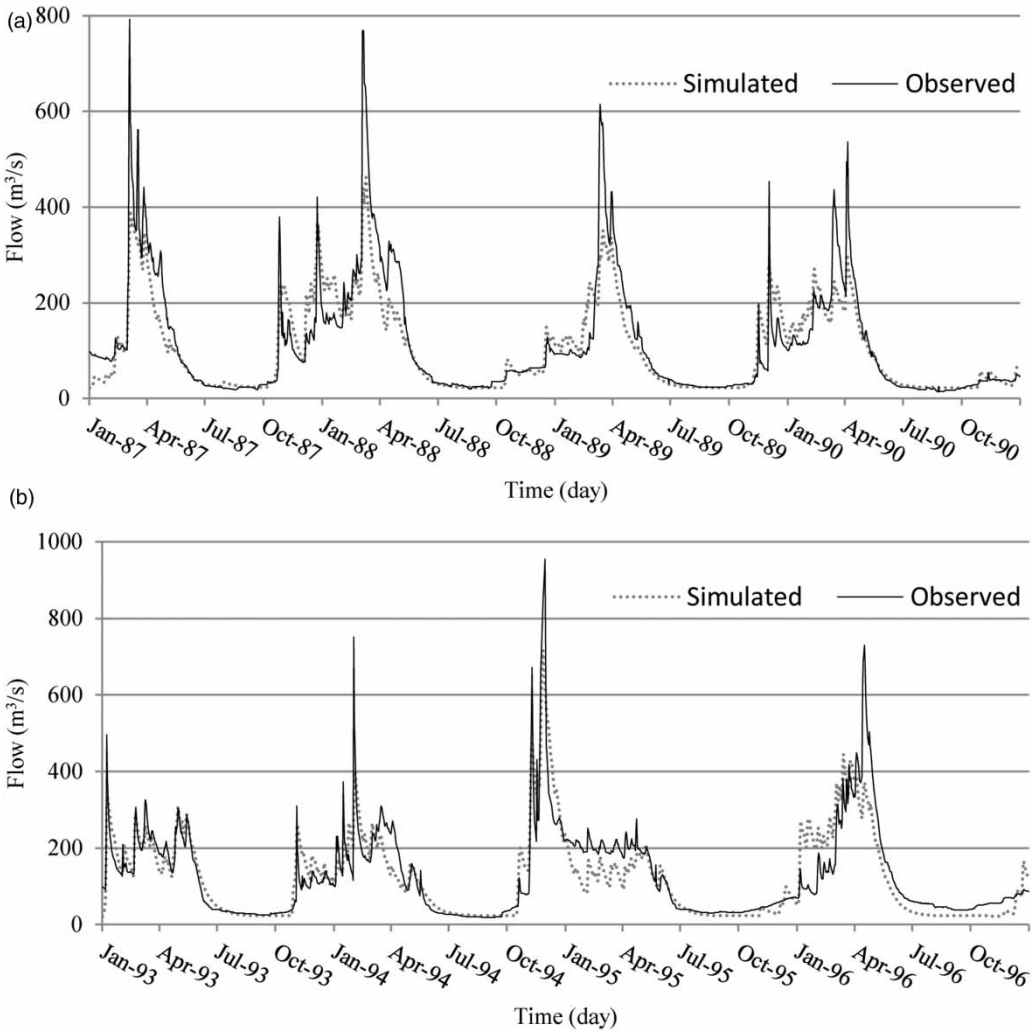

Figure 5 | Comparison of observed and simulated daily inflow to Seimareh Dam: (a) calibration period and (b) validation period.

Table 9 | The mean annual inflow to Seimareh Dam in the 50–year observation and future periods (m^3/s)

	Future period									
	CanESM2						HadCM3			
Observation period	RCP8.5		RCP4.5		RCP2.6		B2		A2	
102.8	89	−13.4%	93.4	−9.1%	97.5	−5.2%	95.6	−7.0%	93	−9.5%

scenario predicts a decrease in energy production of about 16.3% (136.1 GWh): this reduction is remarkable, as it is sufficient power for about 47,000 people in a year. The decline of energy production at Seimareh Hydropower Plant shows its vulnerability in the face of climate change and poses problems for the power grid.

Figure 7 indicates monthly total energy generation by the hydropower plant for the 50-year observation and the

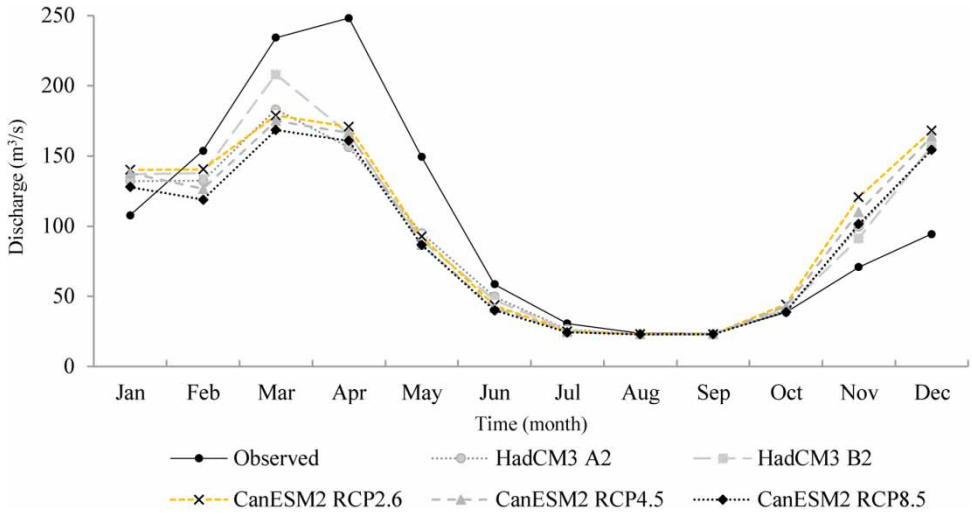

Figure 6 | The mean monthly inflow to Seimareh Dam in the 50–year observation and future periods.

Table 10 | Comparison of annual energy generation by the hydropower plant for future and 50-year observation periods (GWh)

	Future period									
	CanESM2						HadCM3			
Observation period	RCP8.5		RCP4.5		RCP2.6		B2		A2	
832.6	696.5	−16.3%	725.2	−12.9%	762.6	−8.4%	742.1	−10.9%	725.8	−12.8%

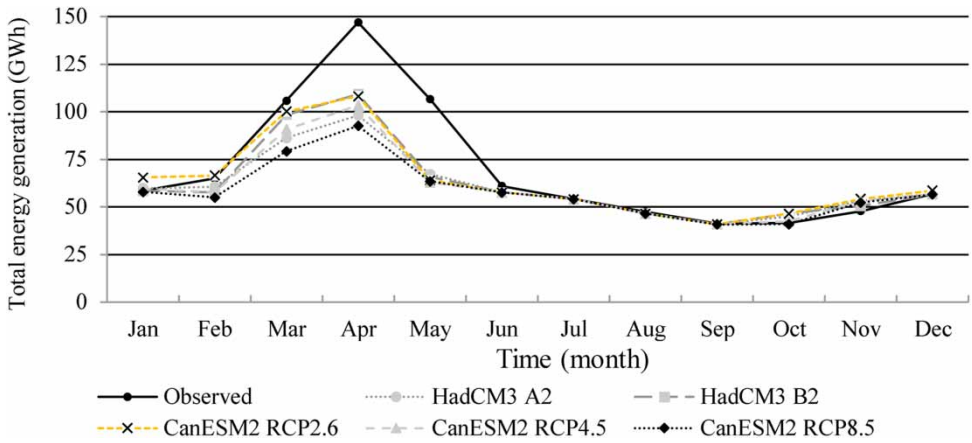

Figure 7 | The mean monthly total energy generation by the hydropower plant for future and 50-year observation periods.

future periods. It can be clearly seen that the amount of total energy generation with various climate models and emission scenarios will change in several months during the future period.

As seen in Figure 7, hydropower production will be influenced by climate change in the future. This phenomenon will alter the amount of energy generated during several months of the year. It is predicted that the Seimareh

plant will experience an increase of 11.8% (7 GWh) under the CanESM2 model and the RCP2.6 scenario during the month of January. The CanESM2 model under the RCP4.5 scenario and the HadCM3 model under the A2 scenario predict a negligible increase (1.7% and 2%, respectively) during this month. The HadCM3 model under the B2 scenario and the CanESM2 model under the RCP8.5 scenario indicate a negligible decrease (0.3% and 1.4%, respectively) for this month. In February, the CanESM2 model under the RCP2.6 scenario is the only case predicting an increase (2.5%). The other models and scenarios estimate reductions of 6.5–15.3% for February. All models and scenarios predict reduced energy generation of between 0.4% and 41% during the period of March to the end of September, with particularly high reduction (37–41%) during May: this amount of decline is considerable. The CanESM2 model under the RCP8.5 scenario is the only case estimating a reduction of 1.2% for October; the other cases predict an increase of 2.2–12.3%. In November, according to the prediction of all models and scenarios, the amount of energy generation will increase between 5.9% and 13.6%. In December, except for the CanESM2 model under RCP2.6, which predicts an increase of 3.2%, an estimated negligible reduction of energy generation is predicted (0.2–0.4%).

CONCLUSIONS

The importance of water and energy resources for human survival is undeniable. Several studies have assessed climate change impacts on the hydropower industry, a very important source of energy. The majority of these studies focus on Europe and the USA. For a better understanding of climate change effects on western Asia, this study tries to assess the performance of Seimareh Dam and Hydropower Plant in the face of climate change. Future climate conditions of the region are predicted using HadCM3 and CanESM2 models under several emission scenarios through the statistical downscaling method. River flow was simulated using the HEC–HMS hydrological model. The expected performance of Seimareh Hydropower Plant was evaluated for a 30-year period (2040–2069) and, using the WEAP model, the amount of hydroelectric energy production under various emission scenarios was assessed. Results show that climate change will influence basin hydrological variables through increased temperatures and reduced precipitation. The Seimareh River flow will decrease under various scenarios in the future. According to various emission scenarios and climate models, the amount of Seimareh Dam inflow will decrease by between 5.2% and 13.4%, relative to the 50-year observation period (1956–2005). River flow patterns will also change. These altered Seimareh River flow patterns and the decreased Seimareh Dam inflow will influence the performance of Seimareh Hydropower Plant. The study estimates that the mean annual total energy production will decrease by 8.4–16.3% under various emission scenarios compared with the 50-year observation period. These outcomes indicate that study and design of hydropower projects should not be based solely on observation data: in this case it is expected that several hydropower plants will face considerable challenges in energy supply. Sufficient attention to climate change should be incorporated into the design and maintenance of water projects: evaluating the anticipated impacts of climate change on various regional water resources can help improve water and energy securities. The present study uses only two climate models and five emission scenarios to assess the future performance of Seimareh Hydropower Plant. It is suggested that the performance of this plant also be assessed using a variety of climate models and emission scenarios in supplementary studies. A wide range of possible scenarios should be evaluated and appropriate management measures taken to prevent adverse conditions in the future.

DATA AVAILABILITY STATEMENT

Data cannot be made publicly available; readers should contact the corresponding author for details.

REFERENCES

Bates, B. C., Kundzewicz, Z. W., Wu, S. & Palutikof, J. P. 2008 *Climate Change and Water*. Technical Paper VI, Intergovernmental Panel on Climate Change Secretariat, Geneva, Switzerland.

Boadi, S. A. & Owusu, K. 2019 Impact of climate change and variability on hydropower in Ghana. *African Geographical Review* **38** (1), 19–31.

Collins, M., Knutti, R., Arblaster, J., Dufresne, J.-L., Fichefet, T., Friedlingstein, P., Gao, X., Gutowski, W. J., Johns, T., Krinner, G., Shongwe, M., Tebaldi, C., Weaver, A. J. & Wehner, M. 2013 Long-term climate change: projections, commitments and irreversibility. In: *Climate Change 2013: The Physical Science Basis. Contribution of Working Group I to the Fifth Assessment Report of the Intergovernmental Panel on Climate Change* (T. F. Stocker, D. Qin, G.-K. Plattner, M. Tignor, S. K. Allen, J. Boschung, A. Nauels, Y. Xi, V. Bex & P. M. Midgley, eds), Cambridge University Press, Cambridge, United Kingdom and New York, NY, USA, pp. 1029–1136.

Fan, J. L., Hu, J. W., Zhang, X., Kong, L. S., Li, F. & Mi, Z. 2020 Impacts of climate change on hydropower generation in China. *Mathematics and Computers in Simulation* **167**, 4–18.

Forrest, K., Tarroja, B., Chiang, F., AghaKouchak, A. & Samuelsen, S. 2018 Assessing climate change impacts on California hydropower generation and ancillary services provision. *Climatic Change* **151**, 395–412.

Ghafouri, M. R., Taheri Shahraiyni, H. & Saghafian, B. 2013 Modeling of continuous daily runoff of Karoon River using SMA loss function. *Iran-Water Resources Research* **9** (2), 73–77.

Halstead, M., Kober, T. & van der Zwaan, B. 2014 *Understanding the Energy–Water Nexus*. ECN-E–14-046, ECN, Petten, The Netherlands.

Hamududu, B. & Killingtveit, Å. 2016 Hydropower production in future climate scenarios: the case for Kwanza River, Angola. *Energies* **9** (5), 363.

Hasan, M. M. & Wyseure, G. 2018 Impact of climate change on hydropower generation in Rio Jubones Basin, Ecuador. *Water Science and Engineering* **11** (2), 157–166.

HEC 2000 *Hydrologic Modeling System HEC–HMS: Technical Reference Manual*. US Army Corps of Engineers, Hydrologic Engineering Center, Davis, CA, USA.

IPCC 2000 *Emissions Scenarios*. Special Report of IPCC Working Group III, Cambridge University Press, Cambridge, UK.

IWPRDC 2008 *Studies of Seimareh Dam & Hydropower Plant.* Iran Water and Power Resources Development Company.

Jalali, M. R., Azaranfar, A. & Afzali, R. 2008 Development of hydropower capabilities in WEAP integrated water resources software. In: *3rd Conference on Water Resource Management*, Tabriz, Iran.

Lehner, B., Czisch, G. & Vassolo, S. 2005 The impact of global change on the hydropower potential of Europe: a model-based analysis. *Energy Policy* **33**, 839–855.

Liu, B., Lund, J. R., Liu, L., Liao, S., Li, G. & Cheng, C. 2020 Climate change impacts on hydropower in Yunnan, China. *Water* **12**, 197.

Lobanova, A., Koch, H., Liersch, S., Hattermann, F. F. & Krysanova, V. 2016 Impacts of changing climate on the hydrology and hydropower production of the Tagus River basin. *Hydrological Processes* **30**, 5039–5052.

Loucks, D. P. & van Beek, E. 2005 *Water Resources Systems Planning and Management: An Introduction to Methods, Models and Applications*. Studies and Reports in Hydrology, UNESCO Publishing, Paris, France.

Maas, A., Issayeva, G., Rüttinger, L., Umirbekov, A. & Daussa, R. 2012 *Climate Change and the Water–Energy–Agriculture Nexus in Central Asia*. Adelphi, Berlin, Germany.

Maran, S., Volonterio, M. & Gaudard, L. 2014 Climate change impacts on hydropower in an alpine catchment. *Environmental Science & Policy* **43**, 15–25.

Meng, Y., Liu, J., Leduc, S., Mesfun, S., Kraxner, F., Mao, G., Qi, W. & Wang, Z. 2020 Hydropower production benefits more from 1.5 °C than 2 °C climate scenario. *Water Resources Research* **55**, e2019WR025519.

Mohtar, R. H. 2017 A call for a new business model valuing water use and production: the water, energy and food nexus holistic system approach. *Water International* **42** (6), 773–776.

Oyerinde, G. T., Wisser, D., Hountondji, F. C. C., Odofin, A. J., Lawin, A. E., Afouda, A. & Diekkrüger, B. 2016 Quantifying uncertainties in modeling climate change impacts on hydropower production. *Climate* **4**, 34.

Qin, P., Xu, H., Liu, M., Du, L., Xiao, C., Liu, L. & Tarroja, B. 2020 Climate change impacts on Three Gorges Reservoir impoundment and hydropower generation. *Journal of Hydrology* **580**, 123922.

Ravazzani, G., Valle, F. D., Gaudard, L., Mendlik, T., Gobiet, A. & Mancini, M. 2016 Assessing climate impacts on hydropower production: the case of the Toce River Basin. *Climate* **4**, 16.

Sieber, J. & Purkey, D. 2015 *User Guide for Water Evaluation And Planning System (WEAP)*. Stockholm Environment Institute, US Center, Somerville, MA, USA.

Spalding-Fecher, R., Joyce, B. & Winkler, H. 2017 Climate change and hydropower in the Southern African Power Pool and Zambezi River Basin: system-wide impacts and policy implications. *Energy Policy* **103**, 84–97.

Tavanir Organization 2016 *Detailed Statistics of Iran's Power Industry for Strategic Management*. Tavanir Organization. Available from: http://amar.tavanir.org.ir.

Teymouri Moghadam, A., Rahnama, G. & Ahmadian, M. 2010 HEC-HMS model calibration for rainfall–runoff simulation of Mahidasht Basin. In: *The National Conference on Water Crisis Management*.

Turner, S. W. D., Ng, J. Y. & Galelli, S. 2017 Examining global electricity supply vulnerability to climate change using a high-fidelity hydropower dam model. *Science of the Total Environment* **590–591**, 663–675.

USDOE 2013 *Effects of Climate Change on Federal Hydropower*. Report to Congress, United States Department of Energy, Washington, DC, USA.

Vicuña, S., Dracup, J. A. & Dale, L. 2011 Climate change impacts on two high-elevation hydropower systems in California. *Climate Change* **109**, 151–169.

Wilby, R. L., Dawson, C. W. & Barrow, E. M. 2002 SDSM – a decision support tool for the assessment of regional climate change impacts. *Environmental Modelling & Software* **17**, 145–157.

Wilby, R. L., Charles, S. P., Zorita, E., Timbal, B., Whetton, P. & Mearns, L. O. 2004 *Guidelines for Use of Climate Scenarios Developed from Statistical Downscaling Methods*. Technical Report, Data Distribution Center of the IPCC.

Zahabiyoun, B., Goodarzi, M. R., Massah Bavani, A. R. & Azamathulla, H. M. 2013 Assessment of climate change impact on the Gharesou River Basin using SWAT hydrological model. *Clean – Soil, Air, Water* **41**, 601–609.

First received 8 October 2019; accepted in revised form 27 June 2020. Available online 10 July 2020